Transient Analysis of Variable-Speed Wind Turbines during a Converter Control Malfunction

R. Melício, V. M. F. Mendes, J. P. S. Catalão

***Abstract*--This paper is on variable-speed wind turbines with permanent magnet synchronous generator. A three-mass drive train model and two different topologies for the power-electronic converters are considered, respectively a two-level and a multilevel converter. A control strategy, based on fractional-order controllers, is proposed for the wind turbines. Simulation results are presented to illustrate the behavior of the wind turbines during a converter control malfunction, considering the fractional-order controllers. Finally, conclusions are duly drawn.**

***Keywords*: computer simulation, power electronics, transient analysis, wind turbines.**

I. Introduction

As the penetration level of wind power increases into the power systems, the overall performance of the electric grid will increasingly be affected by the characteristics of wind turbines. One of the major concerns related to the high penetration level of the wind turbines is the impact on power system stability [1]. Also, network operators have to ensure that consumer power quality is not deteriorated. Hence, the total harmonic distortion (THD) should be kept as low as possible, improving the quality of the energy injected into the electric grid [2]. Power-electronic converters have been developed for integrating wind power with the electric grid. The use of power-electronic converters allows not only for variable-speed operation of a wind turbine, but also for enhancement on power extraction [3].

In a variable-speed wind turbine with full-power converter, the wind turbine is directly connected to the generator and the generator is completely decoupled from the electric grid. Of all the generators used in wind turbines, the permanent magnet synchronous generator (PMSG) is the one with a significant advantage: it is stable and secure under normal operating conditions; and comparing with a wound synchronous generator, it is smaller and does not need a direct current power source for field excitation.

The work of R. Melício was supported by the Fundação para a Ciência e a Tecnologia (FCT) under Post-Doctoral grant (SFRH/BPD/68585/2010).

R. Melício is with Center for Innovation in Electrical and Energy Engineering (CIEEE), IST, Lisbon, and Centre for Aerospace Science and Technologies (CAST), UBI, Covilha, Portugal.

V. M. F. Mendes is with ISEL, Lisbon, and CAST-UBI, Covilha, Portugal.

J. P. S. Catalão is with UBI, Covilha, and CIEEE-IST, Lisbon, Portugal (e-mail of corresponding author: catalao@ubi.pt).

Paper submitted to the International Conference on Power Systems Transients (IPST2011) in Delft, the Netherlands June 14-17, 2011

Accurate modeling and control of wind turbines have high priority in the research activities all over the world. At the moment, substantial documentation exists on modeling and control issues for the doubly fed induction generator (DFIG) wind turbine. But this is not the case for wind turbines with PMSG and full-power converter [4].

Previous papers were mainly focused on the transient analysis of variable-speed wind turbines at external grid faults [5, 6]. However, little attention has been given to the possibility of internal abnormal operating conditions.

The influence of a pitch control malfunction, on the quality of the energy injected into the grid, was studied in [7]. This paper focuses on the transient analysis of wind turbines with PMSG and full-power converters, considering: (i) a three-mass drive train model; (ii) two different topologies for power-electronic converters, respectively two-level and multilevel converters; (iii) a fractional-order control strategy; (iv) a converter control malfunction; (v) the bending flexibility of the blades. Simulation results for the converter control malfunction ascertain the performance of wind turbines equipped with fractional-order controllers.

II. Modeling

A. Wind Turbine

The mechanical power of the turbine is given by:

$$P_{tt} = \frac{1}{2}\rho\pi R^2 u^3 c_p \tag{1}$$

where ρ is the air density, R is the radius of the area covered by the blades, u is the wind speed value, and c_p is the power coefficient.

The computation of the power coefficient requires the use of blade element theory and the knowledge of blade geometry. In this paper, the numerical approximation developed in [8] is followed, where the power coefficient is given by:

$$c_p = 0.73\left(\frac{151}{\lambda_i} - 0.58\theta - 0.002\theta^{2.14} - 13.2\right)e^{-\frac{18.4}{\lambda_i}} \tag{2}$$

$$\lambda_i = \frac{1}{\frac{1}{(\lambda - 0.02\theta)} - \frac{0.003}{(\theta^3 + 1)}} \tag{3}$$

where θ is the pitch angle of the rotor blades and λ is the tip speed ratio.

The global maximum for the power coefficient is at null pitch angle and it is equal to:

$$c_{p\max}(\lambda_{opt}(0),0)=0.4412 \tag{4}$$

corresponding to an optimal tip speed ratio at null pitch angle equal to:

$$\lambda_{opt}(0)=7.057 \tag{5}$$

The conversion of wind energy into mechanical energy over the rotor of a wind turbine is influenced by various forces acting on the blades and on the tower of the wind turbine (e.g. centrifugal, gravity and varying aerodynamic forces acting on blades, gyroscopic forces acting on the tower), introducing mechanical effects influencing the energy conversion [9]. Those mechanical effects have been modeled by eigenswings mainly due to the following phenomena: asymmetry in the turbine, vortex tower interaction, and eigenswing in the blades.

The mechanical power over the rotor of the wind turbine has been modeled, using the mechanical eigenswings [10], as a set of harmonic terms multiplied by the power associated with the energy capture from the wind by the blades, given by:

$$P_t = P_{tt}\left[1+\sum_{k=1}^{3}A_k\left(\sum_{m=1}^{2}a_{km}\ g_{km}(t)\right)h_k(t)\right] \tag{6}$$

$$g_{km}=\sin\left(\int_0^t m\ \omega_k(t')\,dt'+\varphi_{km}\right) \tag{7}$$

where P_t is the mechanical power of the wind turbine disturbed by the mechanical eigenswings, m is the order of the harmonic of a eigenswing, A_k is the magnitude of the eigenswing k, g_{km} is the distribution of the m-order harmonic in the eigenswing k, a_{km} is the normalized magnitude of g_{km}, h_k is the modulation of eigenswing k, ω_k is the eigenfrequency of the eigenswing k, and φ_{km} is the phase of the m-order harmonic in the eigenswing k.

The frequency range of the wind turbine model with mechanical eigenswings is from 0.1 to 10 Hz. The values used on (6) and (7) for the calculation of P_t are given in Table I [10].

TABLE I
MECHANICAL EIGENSWINGS EXCITED IN THE WIND TURBINE

k	Source	A_k	ω_k	h_k	m	a_{km}	φ_{km}
1	Asymmetry	0.01	ω_t	1	1	4/5	0
					2	1/5	π/2
2	Vortex tower interaction	0.08	$3\,\omega_t$	1	1	1/2	0
					2	1/2	π/2
3	Blades	0.15	9 π	1/2 (g_{11}+g_{21})	1	1	0

B. Three-Mass Drive Train Model

With the increase in size of the wind turbines, one question arises whether long flexible blades have an important impact on the transient analysis of wind energy systems during a fault [11].

To determine the dynamic properties of the blade, finite element techniques may be used but this approach cannot easily be implemented in power systems analysis programs. Hence, to avoid the use of the finite element approach it is necessary to simplify the rotor dynamics as much as possible. One way to achieve this is represented in Fig. 1, where the blade analysis is represented as a simple torsional system.

Since the blade bending occurs at a significant distance from the joint between the blade and the hub, the blade can be split in two parts, OA and AB. The blade sections OA1, OA2 and OA3 establish the moment of inertia of the hub and the rigid section blade and have the moment of inertia J_h, the rest of the blade sections A1B1, A2B2 and A3B3 are the effective flexible blade section and have the moment of inertia J_b [12].

The configuration of the three-mass drive train model is shown in Fig. 2. The equations for the three-mass model are based on the torsional version of the second law of Newton, deriving the state equation for the rotor angular speed at the wind turbine and for the rotor angular speed at the generator.

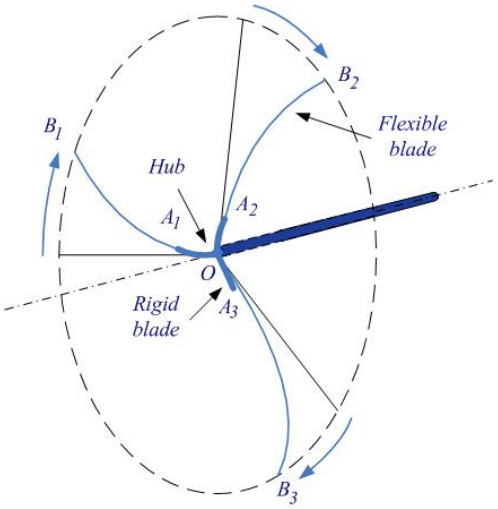

Fig. 1. Blade bending dynamics for the three-mass drive train model.

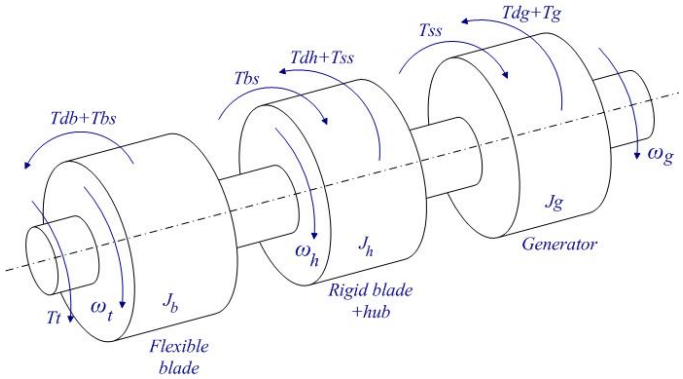

Fig. 2. Blade bending dynamics for the three-mass drive train model.

C. Wind Speed

The wind speed usually varies considerably and it has been modeled in this paper as a sum of harmonics with frequency range 0.1–10 Hz [10].

The wind speed model upstream of the rotor is modeled in this paper by:

$$u(t) = u_0 \left[1 + \sum_k A_k \sin(\omega_k \, t) \right] \tag{8}$$

where u_0 is the average wind speed and u is the wind speed value with disturbance.

D. Generator

The generator considered in this paper is a PMSG. The equations for modeling a PMSG can be found in the literature [13]. In order to avoid demagnetization of permanent magnet in the PMSG, a null stator current is imposed [14].

E. Two-level Converter

The two-level converter is an AC-DC-AC converter, with six unidirectional commanded IGBTs used as a rectifier, and with the same number of unidirectional commanded IGBTs used as an inverter. The rectifier is connected between the PMSG and a capacitor bank. The inverter is connected between this capacitor bank and a second order filter, which in turn is connected to an electric grid. A three-phase active symmetrical circuit in series models the electric grid, as in [7].

The configuration of the wind energy system with two-level converter is shown in Fig. 3.

F. Multilevel Converter

The multilevel converter is an AC-DC-AC converter, with twelve unidirectional commanded IGBTs used as a rectifier, and with the same number of unidirectional commanded IGBTs used as an inverter. The rectifier is connected between the PMSG and a capacitor bank. The inverter is connected between this capacitor bank and a second order filter, which in turn is connected to an electric grid. A three-phase active symmetrical circuit in series models the electric grid, as in [7].

The configuration of the wind energy system with multilevel converter is shown in Fig. 4.

III. Control Strategy

A. Fractional-Order Controller

A control strategy based on fractional-order PI^{μ} controllers is studied for the variable-speed operation of wind turbines with PMSG and full-power converters, and its design is more complex than that of classical PI controllers [15]. Fractional-order calculus used in mathematical models of the systems can improve the design, properties and controlling abilities in dynamical systems [16].

The fractional-order differentiator can be denoted by a general operator ${}_a D_t^{\mu}$ [17], given by:

$${}_a D_t^{\mu} = \begin{cases} \dfrac{d^{\mu}}{dt^{\mu}}, & \Re(\mu) > 0 \\ 1, & \Re(\mu) = 0 \\ \displaystyle\int_a^t (d\tau)^{-\mu}, & \Re(\mu) < 0 \end{cases} \tag{9}$$

where μ is the order of derivative or integrals, $\Re(\mu)$ is the real part of the μ. The mathematical definition of fractional derivatives and integrals has been the subject of several descriptions. The most frequently encountered one is called Riemann–Liouville definition, in which the fractional-order integral is given by:

$${}_a D_t^{-\mu} \, f(t) = \frac{1}{\Gamma(\mu)} \int_a^t (t-\tau)^{\mu-1} f(\tau) \, d\tau \tag{10}$$

while the definition of fractional-order derivatives is:

$${}_a D_t^{\mu} \, f(t) = \frac{1}{\Gamma(n-\mu)} \frac{d^n}{dt^n} \left[\int_a^t \frac{f(\tau)}{(t-\tau)^{\mu-n+1}} \, d\tau \right] \tag{11}$$

where:

$$\Gamma(x) \equiv \int_0^{\infty} y^{x-1} \, e^{-y} \, dy \tag{12}$$

is the Euler's Gamma function, a and t are the limits of the operation, and μ is the number identifying the fractional order. In this paper, μ is assumed as a real number that satisfies the restrictions $0 < \mu \le 1$. Also, it is assumed that $a = 0$. The following convention is used: ${}_0 D_t^{-\mu} \equiv D_t^{-\mu}$.

The differential equation of the fractional-order PI^{μ} controller, $0 < \mu < 1$, in time domain, is given by:

$$u(t) = K_p \, e(t) + K_i \, D_t^{-\mu} \, e(t) \tag{13}$$

where K_p is a proportional constant and K_i is an integration constant. Taking $\mu = 1$ in (13), a classical PI controller is obtained. Hence, using Laplace transforms the transfer function of the fractional-order PI^{μ} controller is given by:

$$G(s) = K_p + K_i \, s^{-\mu} \tag{14}$$

B. Converters Control

Power converters are variable structure systems, because of the on/off switching of their IGBTs. As mentioned previously, the controllers used in the converters are respectively proportional integral and fractional-order PI^{μ} controllers. Pulse width modulation (PWM) by space vector modulation (SVM) associated with sliding mode is used for controlling the converters.

The sliding mode control strategy presents attractive features such as robustness to parametric uncertainties of the wind turbine and the generator as well as to electric grid disturbances [18].

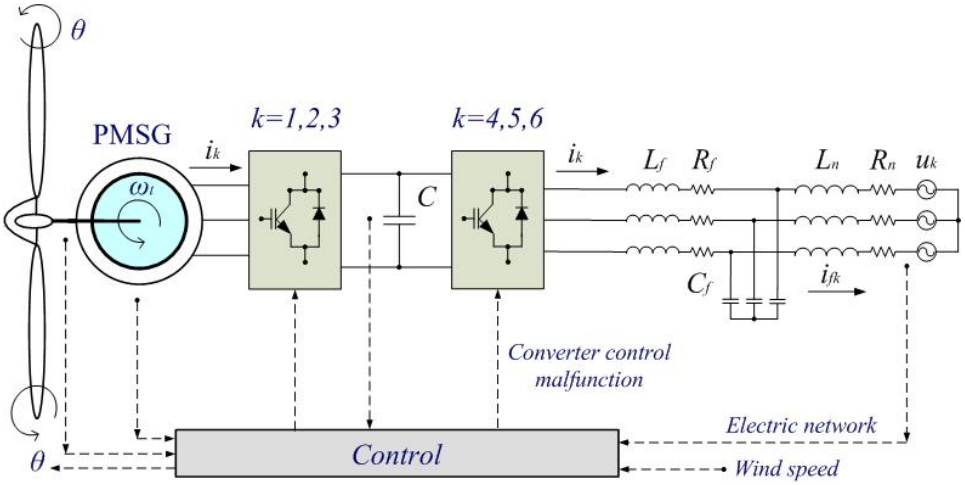

Fig. 3. Wind energy system with two-level converter.

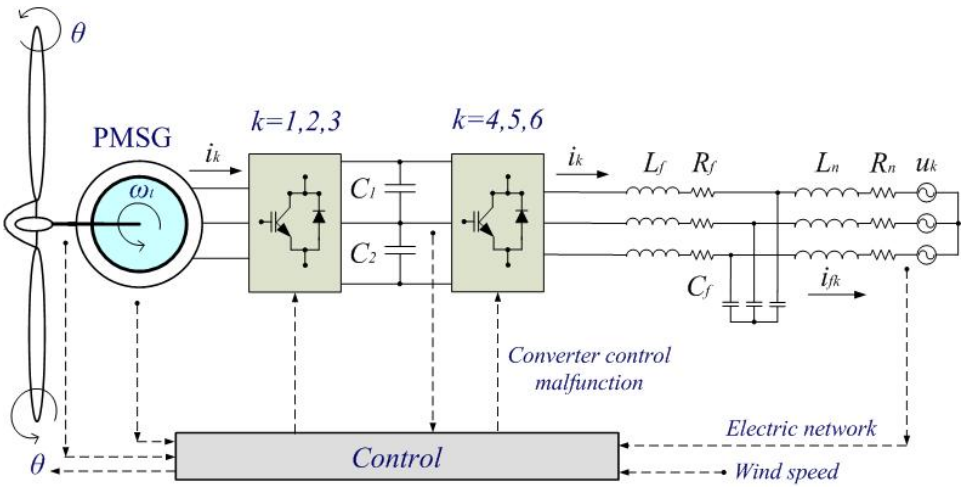

Fig. 4. Wind energy system with multilevel converter.

Although wind turbines achieve an excellent technical availability of about 98% on average, they have to face a high number of malfunctions [19]. A severe malfunction in the control can occur due to voltage sags and swells, harmonics, frequency variation, phase steps, DC components and noise [20].

IV. Simulation

The mathematical models for the wind energy system with the two-level and multilevel converters were implemented in Matlab/Simulink. The wind energy system considered has a turbine rated power of 900 kW. The time horizon considered in the simulation is 10 s. For the fractional-order PI^{μ} controllers, $\mu = 0.7$ is assumed in this paper. Table II summarizes the wind energy system data.

A converter control malfunction is assumed to occur between 7.00 and 7.02 s, imposing a momentary malfunction on the vector selection for the inverter of the two-level and the multilevel converters, simulated by a random selection of vectors constrained to no short circuits on the converters.

The voltage v_{dc} at the capacitor bank for the two-level converter with three-mass drive train model is shown in Fig. 5.

TABLE II
Wind Energy System Data

Blades moment of inertia	400×10^3 kgm²
Hub moment of inertia	19.2×10^3 kgm²
Generator moment of inertia	16×10^3 kgm²
Stiffness	1.8×10^6 Nm
Turbine rotor diameter	49 m
Tip speed	17.64-81.04 m/s
Rotor speed	6.9-30.6 rpm
Turbine rated power	900 kW
Electric generator efficiency	90 %
Number of pairs of poles	10
Stator and rotor resistances	0.042 pu
Stator reactances X_d	1.05 pu
Stator reactances X_q	0.75 pu
Electric grid resistance R_n	0.014 pu
Electric grid reactance X_n	0.175 pu
Inertia constant H	2.2 s

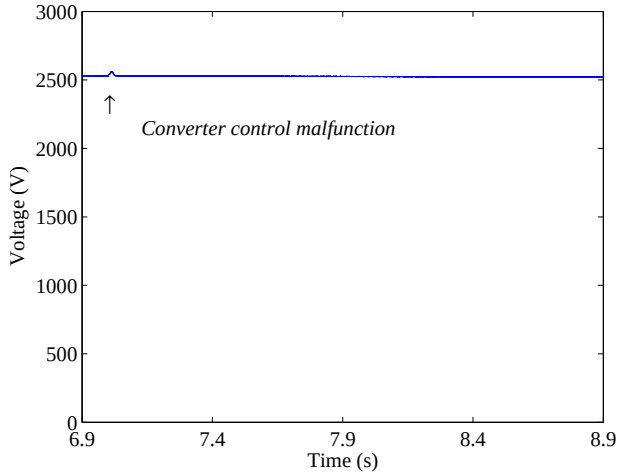

Fig. 5. Voltage v_{dc} for the two-level converter with three-mass drive train model.

As expected during the malfunction the voltage v_{dc} suffers a small increase, the capacitor bank is charged, but almost after the end of the malfunction it recovers to its normal value.

The currents injected into the electric grid for the wind energy system with two-level converter and with the three-mass drive train model are shown in Fig. 6.

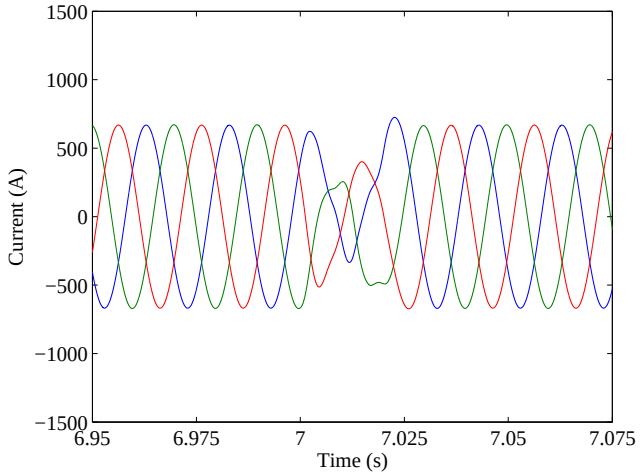

Fig. 6. Currents injected into the electric grid (two-level converter and three-mass drive train model).

As expected during the malfunction the currents injected into the electric grid decrease, but almost after the end of the malfunction they recover to their normal behavior.

The behavior of the voltage v_{dc} at the capacitor banks for the multilevel converter with three-mass drive train model is identical to the behavior with the two-level converter, as shown in Fig. 7.

Also, Fig. 7 shows the inherent neutral-point voltage balancing problem with the multilevel converters due to the capacitor bank voltage divider: one capacitor bank being overcharged, and the other being discharged; additional information can be found in [21, 22].

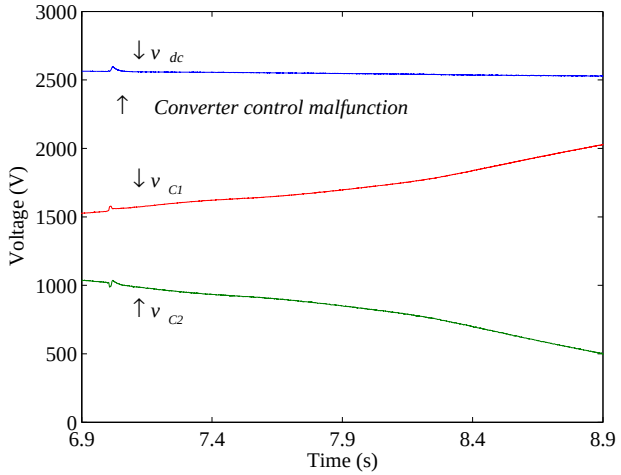

Fig. 7. Voltage v_{dc} for the multilevel converter with three-mass drive train model.

The currents injected into the electric grid for the wind energy system with multilevel converter and with the three-mass drive train model are shown in Fig. 8.

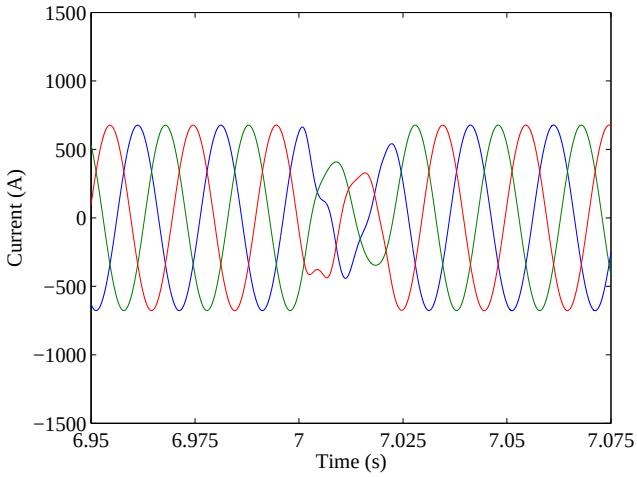

Fig. 8. Currents injected into the electric grid (multilevel converter and three-mass drive train model).

As expected during the malfunction they decrease, but almost after the end of the malfunction they recover to their normal behavior.

It should be noted that, for the same fault conditions, the transient response of the three-mass drive train model is larger than that of the one-mass or the two-mass model. Thus, the three-mass model provides a more realistic approach. The consideration of the bending flexibility of blades can influence the wind turbine response during internal faults.

V. Conclusions

This paper reports a study for PMSG variable-speed wind turbines, considering a three-mass drive train models and two different topologies for the power-electronic converters. Our study deals with the transient analysis during an internal

fault, namely a converter control malfunction. The contributions of this paper are threefold: ascertaining the transient behavior at an internal fault using two-level and multilevel converters; using a control strategy based on fractional-order controllers; and investigating the effects of the bending flexibility of blades. The three-mass drive train model, including both blades and shaft flexibilities, may be more appropriate for the transient analysis of wind energy systems.

VI. References

[1] N. R. Ullah and T. Thiringer, "Variable speed wind turbines for power system stability enhancement," *IEEE Trans. Energy Conversion*, vol. 22, pp. 52-60, Mar. 2007.

[2] J. M. Carrasco, L. G. Franquelo, J. T. Bialasiewicz, E. Galvan, R. C. P. Guisado, A. M. Prats, J. I. Leon, and N. Moreno-Alfonso, "Power-electronic systems for the grid integration of renewable energy sources: A survey," *IEEE Trans. Industrial Electronics*, vol. 53, pp. 1002-1016, Aug. 2006.

[3] J. A. Baroudi, V. Dinavahi, and A. M. Knight, "A review of power converter topologies for wind generators," *Renewable Energy*, vol. 32, pp. 2369-2385, Nov. 2007.

[4] A. D. Hansen and G. Michalke, "Modelling and control of variable-speed multi-pole permanent magnet synchronous generator wind turbine," *Wind Energy*, vol. 11, pp. 537-554, Sep.-Oct. 2008.

[5] C. Jauch, "Transient and dynamic control of a variable speed wind turbine with synchronous generator," *Wind Energy*, vol. 10, pp. 247-269, May-Jun. 2007.

[6] A. H. Kasem, E. F. El-Saadany, H. H. El-Tamaly, and M. A. A. Wahab, "An improved fault ride-through strategy for doubly fed induction generator-based wind turbines," *IET Renew. Power Gener.*, vol. 2, pp. 201-214, Dec. 2008.

[7] R. Melício, V. M. F. Mendes, and J. P. S. Catalão, "Computer simulation of wind power systems: power electronics and transient stability analysis," in: *Proc. IPST 2009*, Kyoto, Japan, Jun. 3-6, 2009.

[8] J. G. Slootweg, S. W. H. de Haan, H. Polinder, and W. L. Kling, "General model for representing variable speed wind turbines in power system dynamics simulations," *IEEE Trans. Power Syst.*, vol. 28, pp. 144-151, Feb. 2003.

[9] Z. X. Xing, Q. L. Zheng, X. J. Yao, and Y. J. Jing, "Integration of large doubly-fed wind power generator system into grid," in: *Proc. 8th Int. Conf. Electrical Machines and Systems,* pp. 1000-1004, Sep. 2005.

[10] V. Akhmatov, H. Knudsen, and A. H. Nielsen, "Advanced simulation of windmills in the electric power supply," *Int. Journal of Electr. Power Energy Syst.*, vol. 22, pp. 421-434, Aug. 2000.

[11] H. Li and Z. Chen, "Transient stability analysis of wind turbines with induction generators considering blades and shaft flexibility," in *Proc. 33rd IEEE IECON*, pp. 1604-1609, 2007.

[12] G. Ramtharan and N. Jenkins, "Influence of rotor structural dynamics representations on the electrical transient performance of DFIG wind turbines," *Wind Energy*, vol. 10, pp. 293-301, Jul.-Aug. 2007.

[13] C.-M. Ong, *Dynamic Simulation of Electric Machinery: Using Matlab/Simulink*. NJ: Prentice-Hall, 1998, pp. 259-350.

[14] T. Senjyu, S. Tamaki, N. Urasaki, and K. Uezato, "Wind velocity and position sensorless operation for PMSG wind generator," in: *Proc. 5th PEDS*, pp. 787-792, Nov. 2003.

[15] B. Arijit, D. Swagatam, A. Ajith, and D. Sambarta, "Design of fractional-order PI-lambda-D-mu-controllers with an improved differential evolution," *Eng. Appl. Artif. Intell.*, vol. 22, pp. 343-350, Mar. 2009.

[16] C. Jun-Yi and C. Bing-Gang, "Design of fractional order controllers based on particle swarm optimization," in: *Proc. IEEE ICIEA* 2006, pp. 1-6, 2006.

[17] A. J. Calderón, B. M. Vinagre, and V. Feliu, "Fractional order control strategies for power electronic buck converters," *Signal Processing*, vol. 86, pp. 2803-2819, Oct. 2006.

[18] B. Beltran, T. Ahmed-Ali, and M. E. H. Benbouzid, "Sliding mode power control of variable-speed wind energy conversion systems," *IEEE Trans. Energy Conversion*, vol. 23, pp. 551-558, Jun. 2008.

[19] B. Hahn, M. Durstewitz, and K. Rohrig, *Reliability of Wind Turbines*, Renewable Energies Knowledge, 2006. Available: www.renknow.net.

[20] A. P. Martins, "A DFT-based phasor estimation method for power electronics converter control and protection under strong grid voltage perturbations," *Eur. Trans. Electr. Power*, vol. 19, pp. 1082-1097, Nov. 2009.

[21] A. Shukla, A. Ghosh, and A. Joshi, "Control schemes for DC capacitor voltages equalization in diode-clamped multilevel inverter-based DSTATCOM," *IEEE Trans. Power Deliv.*, vol. 23, pp. 1139-1149, Apr. 2008.

[22] J.-S. Lai and Z. F. Peng, "Multilevel converters – A new breed of power converters," *IEEE Trans. Ind. Appl.*, vol. 32, pp. 509-517, May-Jun. 1996.